Published in final edited form as:
Osteoporos Int. 2010 February ; 21(2): 263–273. doi:10.1007/s00198-009-0945-7.

Assessment of Trabecular and Cortical Architecture and Mechanical Competence of Bone by High-Resolution Peripheral Computed Tomography: Comparison with Transiliac Bone Biopsy*

A. Cohen[1], **D.W. Dempster**[2], **R. Müller**[3], **X.E. Guo**[1], **T.L. Nickolas**[1], **X.S. Liu**[1], **X.H. Zhang**[1], **A.J. Wirth**[3], **G.H. van Lenthe**[3], **T. Kohler**[3], **D.J. McMahon**[1], **H. Zhou**[2], **M.R. Rubin**[1], **J.P. Bilezikian**[1], **J. M. Lappe**[4], **R.R. Recker**[4], and **E. Shane**[1]

[1]Columbia University, New York, NY, USA [2]Helen Hayes Hospital, West Haverstraw, NY, USA
[3]ETH Zurich, Zurich, Switzerland [4]Creighton University, Omaha, NE, USA

Abstract

Purpose—High resolution peripheral quantitative CT (HR-pQCT) is a new imaging technique that assesses trabecular and cortical bone microarchitecture of the radius and tibia *in vivo*. The purpose of this study was to determine the extent to which microarchitectural variables measured by HR-pQCT reflect those measured by the "gold standard", transiliac bone biopsy.

Methods—HR-pQCT scans (Xtreme CT, Scanco Medical AG) and iliac crest bone biopsies were performed in 54 subjects (aged 39±10 years). Biopsies were analyzed by 2D quantitative histomorphometry and 3D microcomputed tomography (μCT). Apparent Young's modulus, an estimate of mechanical competence or strength, was determined by micro-finite element analysis (μFE) of biopsy μCT and HR-pQCT images.

Results—The strongest correlations observed were between trabecular parameters (bone volume fraction, number, separation) measured by μCT of biopsies and HR-pQCT of the radius (R: 0.365-0.522; $p<0.01$). Cortical width of biopsies correlated with cortical thickness by HR-pQCT, but only at the tibia (R=0.360, $p<0.01$). Apparent Young's modulus calculated by μFE of biopsies correlated with that calculated for both radius (R=0.442; $p<0.001$) and tibia (R=0.380; $p<0.001$) HR-pQCT scans.

Conclusions—The associations between peripheral (HR-pQCT) and axial (transiliac biopsy) measures of microarchitecture and estimated mechanical competence are significant but modest.

Keywords

Bone structure; bone imaging; bone density

Address for Correspondence:, Adi Cohen MD, MHS, Columbia University, College of Physicians & Surgeons, Department of Medicine, PH8-864, 630 West 168th Street, New York, NY 10032, Telephone: 212-342-1291, Telefax: 212-305-3988, ac1044@columbia.edu.

Conflict of Interest Statement:
The authors have no financial relationship with the organizations that sponsored the research, and have no disclosures. The authors have had full control of all primary data and agree to allow the journal to review their data if requested.

INTRODUCTION

Quantitative histomorphometry of transiliac bone biopsy samples is a powerful clinical research tool that has greatly enhanced our understanding of normal bone microstructure, remodeling and strength, as well as the skeletal effects of various diseases and therapies for osteoporosis [13,44]. Both 2-dimensional (2D) histomorphometry of biopsy sections, and more recently, 3-dimensional (3D) micro-computed tomography (μCT) of the entire biopsy specimen have been used to characterize trabecular bone microarchitecture in patients with hyperparathyroidism [11,12,39-41], hypoparathyroidism [46] and osteoporosis [1,21,23], and to document significant improvements in iliac trabecular bone microarchitecture after teriparatide therapy [8,10,34]. In addition, finite element analysis (μFE), a mathematical modeling technique, can be applied to 3D μCT images of biopsy specimens to calculate Young's modulus, an estimate of trabecular bone strength or stiffness that demonstrates excellent agreement with true biomechanical tests of bone specimens [6,25].

As acquisition of iliac crest biopsies is invasive, time-consuming and expensive, there is great interest in noninvasive imaging techniques that permit assessment of bone microstructure *in vivo*. One such noninvasive technique, high-resolution peripheral quantitative computed tomography of the radius and tibia (HR-pQCT; XtremeCT, Scanco Medical AG, Bassersdorf, Switzerland), yields 3D images of sufficiently high resolution (~82 microns) to visualize trabecular microstructure that previously could be assessed only on bone biopsy samples. HR-pQCT provides measurements analogous to those obtained by 2D histomorphometry and 3D μCT of biopsy specimens, including trabecular bone volume fraction (BV/TV), trabecular number (Tb.N), thickness (Tb.Th), and separation (Tb.Sp). However, technical aspects of acquiring the measurements differ among the three techniques, and as the resolution of HR-pQCT is in the range of trabecular dimensions, this technique, in particular, is limited in visualizing individual trabeculae. μFE can be applied to HR-pQCT data sets to estimate mechanical competence *in vivo* [30]. HR-pQCT and μFE of HR-pQCT data sets discriminate between groups of postmenopausal women with and without fractures [3,5,32,48] and may prove useful as a clinical predictor of fracture risk.

MacNeil et al. have demonstrated strong correlations between microarchitecture and strength parameters measured on HR-pQCT scans and μCT and μFE of the same cadaveric radii [30]. However, the relationships between microarchitecture and stiffness measured on transiliac bone biopsies and *in vivo* HR-pQCT scans of the radius and tibia have not been examined. The purpose of this study was to determine the extent to which microarchitectural variables measured by HR-pQCT reflect those measured by the "gold standard", transiliac bone biopsy, in subjects with a broad range of ages, bone mineral density measurements and bone microarchitectural characteristics.

MATERIALS AND METHODS

Study Subjects

We studied 54 subjects who had a percutaneous, transiliac bone biopsy and HR-pQCT scans of the radius and tibia during the course of their participation in one of two research protocols: a cross-sectional case-control study of idiopathic osteoporosis in premenopausal women and a study of bone structure and quality in postsurgical or idiopathic hypoparathyroidism. HR-pQCT scans were performed within 3 ± 3 months of the bone biopsy.

Premenopausal women with osteoporosis were included on the basis of a history of low-trauma fractures or low bone mineral density measurement (T score ≤ −2.5 or Z score ≤ −2.0) at the spine or proximal femur. To qualify as a normal control, women were required

to have normal bone density (T ≥ −1.0 or Z score ≥ −1.0) and no history of fractures. Cases and controls underwent an evaluation to exclude common secondary causes of osteoporosis, including medications, metabolic bone diseases, endocrinopathies, eating disorders, amenorrhea, celiac disease and hypercalciuria. Men and women with hypoparathyroidism had confirmed disease for at least 36 months and were receiving stable therapy with calcium, parent vitamin D and calcitriol.

All subjects were studied at Columbia University Medical Center or Creighton University Medical Center. All subjects provided written informed consent and the Institutional Review Boards of both institutions approved these studies.

Areal bone mineral density (aBMD)

Areal BMD was measured by dual energy x-ray absorptiometry (QDR-4500, Hologic Inc., Walton, MA) at both Columbia and Creighton University Medical Centers, which were cross-calibrated by circulating a phantom between the two sites. Bone density was expressed in terms of T and Z scores for comparisons of subjects with young-normal and age-matched populations, respectively, of the same race and sex.

Transiliac bone biopsy

After double-labeling with tetracycline in a 3:12:3 day sequence, transiliac bone biopsy was performed using a Bordier-type trephine with an inner diameter of 7.5 mm [44]. The biopsy site was 2cm posterior and inferior to the anterior-superior iliac spine. The specimens – an intact core with both cortices and intervening cancellous bone - were fixed and dehydrated in ethanol. After being scanned by μCT, they were embedded in polymethylmethacrylate for 2D quantitative histomorphometry.

Micro-computed tomography

The micro-tomographic imaging system (μCT 40, Scanco Medical AG, Brüttisellen, Switzerland) is equipped with a 5 μm focal spot X-ray tube as a source. A two-dimensional CCD, coupled to a thin scintillator as a detector permits acquisition of 210 tomographic images in parallel. The long axis of the intact biopsy is oriented along the rotation axis of the scanner. The X-ray tube is operated at 50 kVp and 160 μA with an integration time set to 200 ms and all projection frames are recorded 6 times and then averaged. Scans (high resolution mode) are performed at an isotropic, nominal resolution of 8 μm (nominal spatial resolution/voxel size rather than true spatial resolution). For each subject, the intact biopsy was scanned. Biopsies varied in length ranging from 7 mm up to 15 mm, which resulted in measurement times of between 7 and 15 hours. A cylindrical volume of interest was then placed in the digital image data to select the trabecular bone compartment. The mineralized tissue was segmented from soft tissue by a global thresholding procedure [47], with a threshold value set to 34% of the maximum grayscale value. Morphometric indices were determined for the trabecular bone compartment using a direct 3D approach [18] and include bone volume density (BV/TV), Tb.Th, Tb.Sp, and Tb.N.

Bone histomorphometry

After being scanned by μCT, biopsy specimens were embedded, sectioned and stained according to our established procedures [10,13,16,33]. Histomorphometry was performed with a digitizing image-analysis system, consisting of microscopy with normal and UV light, a high-resolution three-chip color video camera, a tablet, a computer and its display, and a morphometric program (OsteoMeasure, Version 4.00C, OsteoMetrics, Inc, Atlanta, GA). All variables were expressed and calculated according to the recommendations of the American Society for Bone and Mineral Research [37].

Conventional indices of bone structure were evaluated on Goldner-stained, 7-μm-thick sections. Before measurements, the cancellous space and cortices were precisely demarcated by well-established criteria [9]. The cancellous bone volume (cancellous bone volume as a percentage of tissue volume; BV/TV), trabecular width (the mean distance across individual trabeculae; Tb.Th), trabecular number [Tb.N; (BV/TV)/Tb.Th], and trabecular separation (the mean distance between individual trabeculae; Tb.Sp) were derived from the two-dimensional (2D) measurement of total tissue area, cancellous bone area, and perimeter using stereological techniques, and assuming a parallel plate model [38]. Cortical width was measured after defining the periosteal and endocortical surfaces. The measurements of bone structure variables were performed at x20 magnification.

HR-pQCT of the radius and tibia

The subjects' nondominant forearm and distal tibia were immobilized in a carbon fiber shell and scanned at Columbia University Medical Center on the Xtreme CT (Scanco Medical AG, Bassersdorf, Switzerland), using manufacturer-defined settings as previously described [3,5,48]. This machine uses a 2D detector array and a 0.08 mm point-focus X-ray tube. The measurement region is first defined on a scout film by manual placement of a reference line at the endplate of the radius or tibia; the first slice is 9.5 mm proximal to the reference line at the radius and 22.5 mm proximal to the reference line at the tibia. A stack of 110 parallel CT slices is then acquired (distal to proximal) at the radius and tibia using an effective energy of 40 keV, slice thickness of 82 microns, image matrix size 1024 × 1024, with a nominal resolution of 82 microns. This provides a 3D image of approximately 9 mm in the axial direction. Attenuation data are converted to equivalent hydroxyapatite (HA) densities. The European Forearm Phantom is scanned at least weekly, or whenever subjects are scanned, for quality control.

The manufacturer's methods of bone microstructure analysis have been described and validated [26-28,35] and applied to several recent clinical studies [3,5,31,32,45,48]. Briefly, the volume of interest (VOI) is automatically separated into cortical and trabecular regions by using a threshold-based algorithm set to one-third the apparent cortical bone density (D_{cort}). Mean cortical thickness (Ct.Th) is defined as the mean cortical volume divided by the outer bone surface. Trabecular bone density (D_{trab}) is defined as the average bone density within the trabecular VOI. BV/TV (%) is derived from D_{trab} assuming that the density of fully mineralized bone is 1.2 g hydroxyapatite/cm^3 (BV/TV = 100 × D_{trab}/1200 mg HA/cm^3). Direct measurements of trabecular microstructure are limited because the nominal spatial resolution of the XtremeCT (82 microns) is in the range of trabecular dimensions; thus visualization of individual trabeculae is limited. Therefore, trabecular structure is assessed using a thickness-independent algorithm [28,29]. Trabecular elements are identified by a mid-axis transformation method and the distance between them is assessed by the distance-transform method [19]. In contrast to 2D histomorphometry, Tb.N is defined as the inverse of the mean spacing of the mid-axes. Tb.Th and Tb.Sp are then derived from BV/TV and Tb.N using formulae derived from traditional quantitative histomorphometry; Tb.Th = (BV/TV)/Tb.N and Tb.Sp = (1- BV/TV)/Tb.N.

μFE of μCT and HR-pQCT images

We used μFE of the μCT images of transiliac bone biopsies and HR-pQCT images from Xtreme CT scans to calculate the apparent Young's modulus (E), an index of resistance to compressive forces (strength or mechanical competence). For μFE of HR-pQCT images, a rectangular volume of interest (VOI) of 70*70*70 voxels, corresponding to 5.74*5.74*5.74 mm^3, was isolated manually from the center of each radius image, and a rectangular VOI of 110*110*110 voxels, corresponding to 9.02*9.02*9.02 mm^3, was isolated manually from the center of each tibia image. The location of the VOI was defined by the center of the

largest cylinder that could fit within the trabecular compartment of tibia and radius, respectively, thus providing a reproducible location based on a customized protocol. Single isolated voxels or a group of connected voxels not connected to the remainder of the trabecular bone network, were removed using component labeling, as they do not contribute mechanically and may cause computational difficulties. The images of VOIs were processed to construct micro finite element models by converting the bone voxels to eight node brick elements. The bone tissue properties were assumed to be isotropic and linearly elastic with a Young's modulus of 15 GPa and a Poisson's ratio of 0.3 for all models [51]. Six μFE analyses, representing three uniaxial compressions and three uniaxial shears, were performed on each model using an element-by-element pre-condition conjugate gradient solver [20,50]. The anisotropic stiffness tensor of each VOI was calculated first in the original image coordinate system. Subsequently, the best-fit orthotropic stiffness matrix and then the principal directions of the stiffness matrix were calculated by minimizing off-diagonal terms and the compliance matrix was transformed to the new principal coordinate system [50]. Based on the compliance matrix, estimated elastic material constants (three apparent Young's moduli, E_{11}, E_{22}, E_{33}) were calculated and sorted. E_{11} represents the modulus along the medial-lateral direction, E_{22} represents the modulus along the anterior-posterior direction, and E_{33} represents the modulus along the longitudinal direction.

Apparent Young's modulus in the long axis (transverse direction) of the biopsies was determined by μFE of μCT images. A rectangular volume of interest of 640*640*300 voxels, corresponding to 5.12*5.12*2.40 mm^3, was isolated in the center of the biopsy image. Images were then converted to finite element models as described for the HR-pQCT images. μFE was restricted to geometric and material linearity. A single load case was applied, representing uniaxial compression along the long axis of the specimen; for the μFE models this is the direction of highest stiffness. For the solution of the resulting systems, a custom in-house parallel conjugate gradient finite element solver with multilevel preconditioning [2] was used.

Statistical analysis

Statistical analyses were performed using SAS software (SAS Institute, Cary NC, USA). All data are expressed as mean + SD. Correlation analyses were conducted to investigate relationships between measures of density, microstructure and mechanics obtained using the different techniques and the different anatomical locations as described above. Pearson correlation coefficients are provided if both parameters were normally distributed and Spearman correlation coefficients are provided if results of one or both parameters were not normally distributed based upon Kolmogorov-Smirnov test (SAS UNIVARIATE procedure). The observed relationships between techniques were not substantially changed by adjustment for age or study group. Therefore the unadjusted data are presented.

RESULTS

Subjects (n=54) included 23 premenopausal women with normal BMD and no fractures, 15 premenopausal women with low BMD or history of low-trauma fracture, and 16 patients with hypoparathyroidism (4 men, 8 premenopausal and 4 postmenopausal women). The average age of the subjects was 39 ± 10 years, with a range of 22 to 65 years. Mean age was 37 ± 8 for normal premenopausal women, 38 ± 9 for premenopausal women with osteoporosis, and 44 ± 12 for subjects with hypoparathyroidism. BMD T-scores ranged from −3.11 to +4.51 (Table 1).

Mean values of lumbar spine and total hip areal BMD and T scores by DXA, trabecular and cortical microstructural parameters assessed at the iliac crest by 2D histomorphometry and 3D μCT, and at the radius and tibia by HR-pQCT are presented in Table 1. Also presented

are mean values of bone stiffness or mechanical competence assessed by μFE of μCT data sets from the iliac crest biopsies (E, in the long axis of the biopsy, transverse) and HR-pQCT scans of the radius and tibia (E_{11}, medial-lateral; E_{22}, anterior-posterior; E_{33}, longitudinal or axial).

At the iliac crest, trabecular microstructural parameters (BV/TV, Tb.N, Tb.Th, and Tb.Sp) assessed by 3D μCT, correlated significantly and strongly with those assessed by 2D histomorphometry (Table 2). Coefficients of correlation (R) ranged from 0.613 to 0.875, all P<0.0001.

Trabecular microstructural parameters assessed by HR-pQCT of the radius and tibia also correlated significantly with each other (Table 2). Correlation coefficients, which ranged from 0.357 to 0.758, were highly significant (P <0.001 to 0.0001), though not as strong than those observed between 2D and 3D histomorphometry at the iliac crest.

In contrast, relationships between trabecular microstructure assessed at the iliac crest by 2D histomorphometry and at the radius and tibia by HR-pQCT were either not significant or only weakly significant (Table 2). At the radius, only BV/TV achieved statistical significance, although there was a trend toward significance for Tb.Sp (p = 0.053). At the tibia, the only near-significant relationship was for BV/TV (p=0.051). Relationships were stronger between 3D μCT of the iliac crest and HR-pQCT of the radius and tibia than with 2D histomorphometry, particularly at the radius, where correlations between BV/TV, Tb.N and Tb.Sp were of moderate strength (R = 0.365 to 0.522; p <0.01 to 0.0001; Table 2 and Figure 1).

Interestingly, correlations between BV/TV measured by 2D histomorphometry at the iliac crest and by peripheral HR-pQCT (R for radius, 0.304; p < 0.05 and for tibia, 0.274; p=NS) were comparable to those between BV/TV by 2D histomorphometry and central areal BMD by DXA (R = 0.274 for lumbar spine and 0.306 for total hip; both p<0.05) (Table 2). DXA was somewhat more strongly associated with BV/TV by 3D μCT (R = 0.352 for lumbar spine and 0.365 for total hip; both p<0.01) than by 2D histomorphometry. In contrast, relationships between BV/TV of the radius and tibia measured by HR-pQCT and central areal BMD were considerably stronger. Radius BV/TV correlated significantly with lumbar spine and total hip aBMD (R = 0.645 and 0.648, respectively, both p<0.0001). Tibia BV/TV also correlated significantly with lumbar spine and total hip aBMD (R = 0.637 and 0. 749, respectively, both p<0.0001). The results were not substantially altered after adjusting for age or age and group (premenopausal control, premenopausal osteoporosis, hypoparathyroidism).

HR-pQCT of the radius and tibia and 2D histomorphometry of biopsy specimens provide measures of cortical thickness and width, respectively (Table 1). Cortical thickness of the radius correlated moderately well with that of the tibia (R = 0.578, p<0.0001; Table 2). However, the relationship between cortical width by 2D histomorphometry and cortical thickness by HR-pQCT of the radius was not significant, and the correlation at the tibia was weak (R=0.360, p <0.01).

Apparent Young's moduli estimated by μFE are shown in Table 1 and representative μFE images from normal, osteoporotic and hypoparathyroid subjects are shown in Figure 2. The strongest relationship was that between μFE of HR-pQCT scans of the radius and tibia in the medial-lateral direction (E_{11}; R=0.615, p<0.0001), while correlations between the anterior-posterior and longitudinal or axial directions were less robust (Table 3). μFE of the transiliac biopsies (E in the long axis of the biopsy or transverse direction) correlated with E_{11} in the medial-lateral direction of HR-pQCT scans of the radius (R=0.442; p<0.001) and tibia (R=0.380; p<0.001). There were also weaker but significant correlations between E of the

biopsy and E_{22} (anterior-posterior) and E_{33} (axial or longitudinal) at the radius, although not at the tibia. Areal BMD by DXA correlated significantly with μFE of HR-pQCT scans but minimally or not at all with μFE of transiliac biopsies. Pearson correlation coefficients ranged from 0.431-0.648 (all $p \leq 0.002$) for lumbar spine and 0.364-0.664 (all $p \leq 0.009$) for total hip BMD versus three Young's moduli of radius and tibia. In contrast, correlations between areal BMD by DXA and μFE of biopsies were weak and of borderline statistical significance ($R = 0.278$; $p=0.05$ and $R = 0.234$, $p=0.1$, for lumbar spine and total hip respectively).

DISCUSSION

This is the first study to evaluate the extent to which trabecular and cortical microarchitectural and strength variables measured by HR-pQCT of the distal radius and tibia reflect those assessed in the same subjects by 2D histomorphometry and 3D μCT of the iliac crest bone biopsy. In a diverse group of subjects characterized by a broad range of ages, bone density measurements and microarchitectural features, we found that measurements made on or derived from HR-pQCT scans of the radius and tibia generally did not correlate with those made by 2D histomorphometry at the iliac crest; only BV/TV achieved statistical significance and only at the radius. Although relationships between HR-pQCT and 3D (volumetric) μCT of the iliac crest were stronger, they were still relatively modest. The relationships between apparent Young's moduli estimated from HR-pQCT of the radius and tibia (in 3 directions) and calculated from μCT scans of the biopsy were of similarly moderate strength. In all cases, relationships were stronger between iliac crest and the radius than the tibia. These results suggest that structural and strength parameters measured by HR-pQCT are largely not predictive of those measured by quantitative 2D histomorphometry and only moderately predictive of 3D μCT at the iliac crest.

Quantitative histomorphometry of transiliac crest bone biopsies is an invaluable tool for the study of dynamic indices of bone remodeling. Additionally, it has long been considered the "gold standard" for evaluating bone microarchitecture. Over the past three decades, it has provided fundamental information about bone microarchitecture in a number of important metabolic bone diseases, including postmenopausal osteoporosis [42], osteoporosis in men [24], primary hyperparathyroidism [40], renal bone disease [15], and more recently, hypoparathyroidism [46] and idiopathic osteoporosis in premenopausal women [14]. More recently, the application of μCT to bone biopsy specimens has improved assessment of trabecular microarchitecture, because the analysis is truly volumetric, encompasses the entire biopsy specimen rather than being limited to several histological sections, and does not rest upon assumptions of the underlying plate- or rod-like nature of trabecular structure.

With the recent introduction of high-resolution, 3D *in vivo* imaging techniques such as micro-MRI and HR-pQCT, it has become possible to assess trabecular microarchitecture non-invasively at clinically relevant weight bearing and non-weight bearing skeletal sites that may be affected by osteoporosis and may predict fracture. In this study, we aimed to determine the degree to which microstructural parameters of peripheral sites assessed by HR-pQCT, sometimes referred to as a "virtual bone biopsy", reflect those measured on biopsy specimens from the iliac crest.

As expected, we observed strong correlations between traditional 2D histomorphometry and 3D μCT of iliac crest biopsies, consistent with previous studies in our laboratories and those of other investigators conducted in populations with a wide range of ages and diverse clinical diagnoses [7,11,22,36,43,49]. Recker et al. found strong relationships between microarchitectural variables measured by both techniques in 88 postmenopausal women, with correlations ranging from 0.60 for trabecular thickness to 0.83 for bone volume [43].

Similarly, we found strong relationships between 2D histomorphometry and 3D μCT in transiliac crest biopsies from 44 men and women with primary hyperparathyroidism, with R values ranging from 0.65 to 0.79 [11], similar to the range we observed in this study (0.61 to 0.88). In this study, we also observed highly significant correlations between trabecular microstructural parameters assessed by HR-pQCT of the radius and tibia.

In contrast to the strong relationships between 2D and 3D assessments of transiliac crest biopsies and between HR-pQCT scans of the radius and tibia, the most robust correlations we observed between biopsy and HR-pQCT parameters, specifically between BV/TV, Tb.N and Tb.Sp measured by μCT of iliac crest biopsies and HR-pQCT, were quite weak at the radius (R^2 = 0.158, 0.133 and 0.273, respectively) and even more so at the tibia (R^2= 0.076, 0.046 and 0.115, respectively), while Tb.Th did not achieve statistical significance at all. Mechanical competence, as assessed by Young's moduli, also correlated weakly between the iliac crest and radius (R^2 = 0.110-0.195) and even more weakly with the tibia (R^2 = 0.013-0.144). Notably, relationships between areal BMD of central sites (lumbar spine and total hip) and BV/TV measured by both 2D histomorphometry and 3D μCT of the iliac crest were also weak, while those between areal BMD and BV/TV by HR-pQCT were much more robust (R^2 = 0.405 - 0.561). The fact that relationships between HR-pQCT (BV/TV of radius and tibia) and DXA measurements of areal BMD (spine and hip) were stronger than those between HR-pQCT and histomorphometry (2D or 3D) of the iliac crest suggests that perhaps it is the iliac crest site *per se* that is the source of the variability and weaker relationships. In this regard, Hildebrand et al. found that trabecular structure at the iliac crest is characterized by large inter-individual differences, with some subjects having a more rod-like and others a more plate-like architecture [18].

The stronger relationships between HR-QCT and 3D μCT than 2D histomorphometric parameters are likely seen both because the 2D data represent only a fraction of the entire biopsy scanned by μCT and also because neither HR-pQCT nor μCT depend upon *a priori* assumptions regarding the plate-like or rod-like nature of the underlying trabecular structure, whereas the stereologic techniques used in 2D histomorphometry are derived assuming a fixed structural model, specifically a parallel plate model. The stronger relationships between μCT and μFE of iliac crest and radius than tibia may be because the tibia is a weight bearing bone, while neither iliac crest nor radius are weight bearing sites. Mechanical stimuli associated with weight bearing may mitigate trabecular microarchitectural changes that accompany aging, gonadal hormone deficiency or diseases that affect the skeleton. In this regard, Boutroy et al. found that HR-pQCT of the radius discriminated between osteopenic women with and without fractures, while the tibia did not [3].

Certain variables measured by HR-pQCT bore stronger relationships to those measured on biopsies than others. BV/TV, which is derived from volumetric BMD, was the most consistently predictive measurement. The correlation between Tb.Sp at the iliac crest measured by μCT and at the radius by HR-pQCT was also relatively strong. Other studies suggest that trabecular separation may be a particularly important determinant of bone strength. In a study comparing 2D-histomorphometry of transiliac biopsies in two groups of women, with and without documented vertebral fractures, the largest between-groups difference was a 49% increase in Tb.Sp [23]. Similarly, in a study comparing 2D histomorphometry and 3D μCT parameters in Japanese women with and without spine fractures, Tb.N was significantly lower and Tb.Sp significantly higher in those with spine fractures [22]. HR-pQCT results are consistent with these biopsy studies; Tb.Sp and heterogeneity of the trabecular network assessed by HR-pQCT discriminated between postmenopausal osteopenic women with and without fractures [3,4].

The relatively weak relationships we observed could also be accounted for by several technical and analytic differences in the measurement of similarly named parameters by μCT, histomorphometry and HR-pQCT, which use different algorithms to calculate parameters of trabecular structure. For example, HR-pQCT derives BV/TV from directly measured trabecular bone density (D_{trab}, the average bone density within the trabecular VOI), assuming that the density of fully mineralized bone is 1.2 g hydroxyapatite/cm^3. BV/TV assessed by 2D histomorphometry is calculated as the volume of trabecular bone (including both mineralized and unmineralized matrix) as a percentage of tissue volume (which includes trabecular bone, marrow and associated soft tissues). In contrast, BV/TV, assessed by μCT, is measured directly and includes only mineralized bone [17]. Similar technical issues likely influenced the relationships among other trabecular microstructural parameters measured by the different techniques. This may be particularly relevant to trabecular thickness, which did not correlate between either 2D histomorphometry or μCT of the biopsy and HR-pQCT of radius or tibia. In this regard, our results are similar to those of Hildebrand et al. who found that Tb.Th was 21-43% lower when calculated by 2D histomorphometry than when measured directly by μCT [18]. Moreover, because the nominal resolution of HR-pQCT, 82 microns, is so similar to trabecular dimensions, partial volume effects limit visualization of individual trabeculae with this technology. In addition, the fact that trabecular thickness is directly measured by μCT with its resolution of <10 μm and is a derived measure for HR-pQCT (nominal resolution, 82 μm) likely affects the results. Thus, despite the fact that similar names and symbols are used to describe parameters obtained using different modalities (eg., TbSp, TbTh), these are really different measurements and there is a clear limitation in comparing them.

Site-to-site differences in bone structure at different anatomical regions likely also contribute to the relatively weak relationships observed in this study. MacNeil et al. found that HR-pQCT accurately reflects μCT and μFE of biopsies taken from the same regions of cadaveric radii [30]. Trabecular parameters (BV/TV, Tb.N, Tb.Th, Tb.Sp) measured by the two imaging techniques correlated well (R^2 = 0.59-0.95), as did mechanical stiffness assessed by μFE of both image types (R^2 = 0.50-0.73) [30]. In contrast, we compared different anatomical sites (iliac crest versus radius or tibia), bones that differ structurally and also are loaded and adapted differently. We are not aware of other clinical studies that have evaluated relationships between either traditional 2D histomorphometry or μCT of iliac crest biopsies and HR-pQCT of the radius and tibia. However, Hildebrand et al. also reported large inter-site trabecular differences between biopsies from different anatomical sites (iliac crest, femoral head, lumbar spine, and calcaneal core) of the same cadavers analyzed by μCT [18].

Our study has several limitations. These include the technical and analytic differences summarized above that characterize the three techniques evaluated and the variability inherent in analyzing bone samples from different anatomic sites, which differ structurally and also in terms of adaptation to differences in loading. Additionally, assumptions of uniform bone mineralization are incorporated into μFE analyses, which could affect results in the varied clinical population studied here. Relatively few subjects had fractures and thus we could not evaluate the extent to which these techniques discriminated between patients with and without fractures.

Our study also has an important strength. To our knowledge, it is the only study to evaluate in the same human subjects, relationships among measurements of areal BMD of the spine and total hip by DXA, bone microstructure and strength assessed on transiliac bone biopsies and HR-pQCT scans of the distal radius and tibia. These different technologies are used to assess bone structure, both in clinical practice and in research, and it is important to understand the differences in the information that they provide. The biological relevance of

HR-pQCT to the central skeleton in the individual patient or for large scale clinical application remains to be determined and will be best assessed as this tool continues to be studied as a predictor of fracture risk. HRpQCT may also prove to be a useful tool to understand structural effects of many metabolic bone disorders and therapeutic maneuvers on the skeleton.

In conclusion, we observed relatively weak and largely non-predictive relationships between transiliac biopsies and HR-pQCT scans, while relationships between HR-pQCT scans and central DXA of the spine and hip were considerably stronger. These results raise several issues that require further consideration. Among the assessment tools evaluated, it is not clear which will ultimately prove to be the best predictor of bone strength and fracture risk and thus which should be considered the gold standard. A much larger study addressing the sensitivity and specificity of transiliac bone biopsy, DXA, HR-pQCT and μFE to discriminate between subjects with and without fractures would be necessary to resolve this issue. Although DXA is the most available and accessible technology, several investigators have demonstrated that microarchitectural parameters measured by HR-pQCT offer improved discrimination between groups of patients with and without fractures [3,5,32,48]. However, it is not clear whether the resolution of HR-pQCT is truly adequate to assess trabecular structure, as it is also possible that the better fracture discrimination documented with the Xtreme CT is really a function of more accurately assessing trabecular versus cortical density. Moreover, the complete lack of any relationship between trabecular thickness measured by any of the techniques brings into question the value of this particular parameter. Finally, although 2D histomorphometry of transiliac biopsy samples is the oldest technique, our results suggest it may not, in fact, be the most representative site to assess trabecular bone structure and strength. Ultimately, the newly available 3D technologies may require us to revisit the results of older studies that used classical 2D histomorphometry.

Mini-Abstract

We compared microarchitecture and mechanical competence parameters measured by high resolution peripheral quantitative CT (HR-pQCT) and finite element analysis of radius and tibia to those measured by histomorphometry, micro-CT and finite element analysis of transiliac bone biopsies. Correlations were weak to moderate between parameters measured on biopsies and scans.

Acknowledgments

These studies are supported by the following NIH funding sources: AR49896, DK069350, and AR051376

Computing time for finite element analysis of the bone biopsies was granted by the Swiss National Supercomputing Centre (CSCS, Manno, Switzerland).

REFERENCES

1. Aaron JE, Shore PA, Shore RC, Beneton M, Kanis JA. Trabecular architecture in women and men of similar bone mass with and without vertebral fracture: II. Three-dimensional histology. Bone 2000;27:277–282. [PubMed: 10913922]
2. Arbenz P, van Lenthe GH, Mennel U, Müller R, Sala M. A scalable multi-level preconditioner for matrix-free micro-finite element analysis of human bone structures. Internat. J. Numer. Methods Engrg 2008;73:927–947. doi:910.1002/nme.2101.
3. Boutroy S, Bouxsein ML, Munoz F, Delmas PD. In vivo assessment of trabecular bone microarchitecture by high-resolution peripheral quantitative computed tomography. J Clin Endocrinol Metab 2005;90:6508–6515. [PubMed: 16189253]

4. Boutroy S, van Rietbergen B, Sornay-Rendu E, Munoz F, Bouxsein ML, Delmas PD. Finite Element Analyses Based on In Vivo HR-pQCT Images of the Distal Radius is Associated with Wrist Fracture in Postmenopausal Women. J Bone Miner Res. 2007
5. Boutroy S, Van Rietbergen B, Sornay-Rendu E, Munoz F, Bouxsein ML, Delmas PD. Finite element analysis based on in vivo HR-pQCT images of the distal radius is associated with wrist fracture in postmenopausal women. J Bone Miner Res 2008;23:392–399. [PubMed: 17997712]
6. Boyd SK, Muller R, Zernicke RF. Mechanical and architectural bone adaptation in early stage experimental osteoarthritis. J Bone Miner Res 2002;17:687–694. [PubMed: 11918226]
7. Chappard D, Retailleau-Gaborit N, Legrand E, Basle MF, Audran M. Comparison insight bone measurements by histomorphometry and microCT. J Bone Miner Res 2005;20:1177–1184. [PubMed: 15940370]
8. Chen P, Miller PD, Recker R, Resch H, Rana A, Pavo I, Sipos AA. Increases in BMD correlate with improvements in bone microarchitecture with teriparatide treatment in postmenopausal women with osteoporosis. J Bone Miner Res 2007;22:1173–1180. [PubMed: 17451369]
9. Courpron, P.; Meunier, PJ.; Bressot, C.; Giroux, JM. In: Meunier, PJ., editor. Amount of bone in iliac crest biopsy: significance of the trabecular bone volume. Its values in normal and pathological conditions; Proc Second International Workshop on Bone Histomorphometry. Society de la Nouvelle Imprimerie Fournie; Toulouse, France. 1976; p. 39-53.
10. Dempster DW, Cosman F, Kurland ES, Zhou H, Nieves J, Woelfert L, Shane E, Plavetic K, Muller R, Bilezikian J, Lindsay R. Effects of daily treatment with parathyroid hormone on bone microarchitecture and turnover in patients with osteoporosis: a paired biopsy study. J Bone Miner Res 2001;16:1846–1853. [PubMed: 11585349]
11. Dempster DW, Muller R, Zhou H, Kohler T, Shane E, Parisien M, Silverberg SJ, Bilezikian JP. Preserved three-dimensional cancellous bone structure in mild primary hyperparathyroidism. Bone 2007;41:19–24. [PubMed: 17490921]
12. Dempster DW, Parisien M, Silverberg SJ, Liang XG, Schnitzer M, Shen V, Shane E, Kimmel DB, Recker R, Lindsay R, Bilezikian JP. On the mechanism of cancellous bone preservation in postmenopausal women with mild primary hyperparathyroidism. J Clin Endocrinol Metab 1999;84:1562–1566. [PubMed: 10323380]
13. Dempster, DW.; Shane, E. Bone quantification and dynamics of bone turnover. In: Becker, KL., editor. Principles and Practice of Endocrinology and Metabolism. Lippincott Co; Philadelphia, PA: 2002. p. 475-479.
14. Donovan MA, Dempster D, Zhou H, McMahon DJ, Fleischer J, Shane E. Low bone formation in premenopausal women with idiopathic osteoporosis. J Clin Endocrinol Metab 2005;90:3331–3336. [PubMed: 15784712]
15. Elder G. Pathophysiology and recent advances in the management of renal osteodystrophy. J Bone Miner Res 2002;17:2094–2105. [PubMed: 12469904]
16. Goldner J. A modification of the Masson trichrome technique for routine laboratory purposes. Am J Pathol 1938;14:237–243. [PubMed: 19970387]
17. Guilak F. Volume and surface area measurement of viable chondrocytes in situ using geometric modelling of serial confocal sections. J Microsc 1994;173:245–256. [PubMed: 8189447]
18. Hildebrand T, Laib A, Muller R, Dequeker J, Ruegsegger P. Direct three-dimensional morphometric analysis of human cancellous bone: microstructural data from spine, femur, iliac crest, and calcaneus. J Bone Miner Res 1999;14:1167–1174. [PubMed: 10404017]
19. Hildebrand T, Ruegsegger P. Quantification of Bone Microarchitecture with the Structure Model Index. Comput Methods Biomech Biomed Engin 1997;1:15–23. [PubMed: 11264794]
20. Hollister SJ, Brennan JM, Kikuchi N. A homogenization sampling procedure for calculating trabecular bone effective stiffness and tissue level stress. J Biomech 1994;27:433–444. [PubMed: 8188724]
21. Hordon LD, Raisi M, Aaron JE, Paxton SK, Beneton M, Kanis JA. Trabecular architecture in women and men of similar bone mass with and without vertebral fracture: I. Two-dimensional histology. Bone 2000;27:271–276. [PubMed: 10913921]

22. Ito M, Nakamura T, Matsumoto T, Tsurusaki K, Hayashi K. Analysis of trabecular microarchitecture of human iliac bone using microcomputed tomography in patients with hip arthrosis with or without vertebral fracture. Bone 1998;23:163–169. [PubMed: 9701476]
23. Kimmel DB, Recker RR, Gallagher JC, Vaswani AS, Aloia JF. A comparison of iliac bone histomorphometric data in post-menopausal osteoporotic and normal subjects. Bone Miner 1990;11:217–235. [PubMed: 2268749]
24. Kurland ES, Rosen CJ, Cosman F, McMahon D, Chan F, Shane E, Lindsay R, Dempster D, Bilezikian JP. Insulin-like growth factor-I in men with idiopathic osteoporosis. J Clin Endocrinol Metab 1997;82:2799–2805. [PubMed: 9284699]
25. Ladd AJ, Kinney JH, Haupt DL, Goldstein SA. Finite-element modeling of trabecular bone: comparison with mechanical testing and determination of tissue modulus. J Orthop Res 1998;16:622–628. [PubMed: 9820288]
26. Laib A, Hauselmann HJ, Ruegsegger P. In vivo high resolution 3D-QCT of the human forearm. Technol Health Care 1998;6:329–337. [PubMed: 10100936]
27. Laib A, Hildebrand T, Hauselmann HJ, Ruegsegger P. Ridge number density: a new parameter for in vivo bone structure analysis. Bone 1997;21:541–546. [PubMed: 9430245]
28. Laib A, Ruegsegger P. Calibration of trabecular bone structure measurements of in vivo three-dimensional peripheral quantitative computed tomography with 28-microm-resolution microcomputed tomography. Bone 1999;24:35–39. [PubMed: 9916782]
29. Laib A, Ruegsegger P. Comparison of structure extraction methods for in vivo trabecular bone measurements. Comput Med Imaging Graph 1999;23:69–74. [PubMed: 10227372]
30. MacNeil JA, Boyd SK. Accuracy of high-resolution peripheral quantitative computed tomography for measurement of bone quality. Med Eng Phys 2007;29:1096–1105. [PubMed: 17229586]
31. Melton LJ 3rd, Riggs BL, Keaveny TM, Achenbach SJ, Hoffmann PF, Camp JJ, Rouleau PA, Bouxsein ML, Amin S, Atkinson EJ, Robb RA, Khosla S. Structural determinants of vertebral fracture risk. J Bone Miner Res 2007;22:1885–1892. [PubMed: 17680721]
32. Melton LJ 3rd, Riggs BL, van Lenthe GH, Achenbach SJ, Muller R, Bouxsein ML, Amin S, Atkinson EJ, Khosla S. Contribution of in vivo structural measurements and load/strength ratios to the determination of forearm fracture risk in postmenopausal women. J Bone Miner Res 2007;22:1442–1448. [PubMed: 17539738]
33. Meunier, PJ.; Bressot, C. Endocrine influences on bone cells and bone remodeling evaluated by clinical histomorphometry. Raven Press; New York, NY: 1983.
34. Miki T, Nakatsuka K, Naka H, Masaki H, Imanishi Y, Ito M, Inaba M, Morii H, Nishizawa Y. Effect and safety of intermittent weekly administration of human parathyroid hormone 1-34 in patients with primary osteoporosis evaluated by histomorphometry and microstructural analysis of iliac trabecular bone before and after 1 year of treatment. J Bone Miner Metab 2004;22:569–576. [PubMed: 15490267]
35. Muller R, Hildebrand T, Hauselmann HJ, Ruegsegger P. In vivo reproducibility of three-dimensional structural properties of noninvasive bone biopsies using 3D-pQCT. J Bone Miner Res 1996;11:1745–1750. [PubMed: 8915782]
36. Muller R, Van Campenhout H, Van Damme B, Van Der Perre G, Dequeker J, Hildebrand T, Ruegsegger P. Morphometric analysis of human bone biopsies: a quantitative structural comparison of histological sections and micro-computed tomography. Bone 1998;23:59–66. [PubMed: 9662131]
37. Parfitt AM, Drezner MK, Glorieux FH, Kanis JA, Malluche H, Meunier PJ, Ott SM, Recker RR. Bone histomorphometry: standardization of nomenclature, symbols, and units. Report of the ASBMR Histomorphometry Nomenclature Committee. J Bone Miner Res 1987;2:595–610. [PubMed: 3455637]
38. Parfitt AM, Mathews CH, Villanueva AR, Kleerekoper M, Frame B, Rao DS. Relationships between surface, volume, and thickness of iliac trabecular bone in aging and in osteoporosis. Implications for the microanatomic and cellular mechanisms of bone loss. J Clin Invest 1983;72:1396–1409. [PubMed: 6630513]

39. Parisien M, Cosman F, Mellish RW, Schnitzer M, Nieves J, Silverberg SJ, Shane E, Kimmel D, Recker RR, Bilezikian JP, et al. Bone structure in postmenopausal hyperparathyroid, osteoporotic, and normal women. J Bone Miner Res 1995;10:1393–1399. [PubMed: 7502712]
40. Parisien M, Mellish RW, Silverberg SJ, Shane E, Lindsay R, Bilezikian JP, Dempster DW. Maintenance of cancellous bone connectivity in primary hyperparathyroidism: trabecular strut analysis. J Bone Miner Res 1992;7:913–919. [PubMed: 1442205]
41. Parisien M, Silverberg SJ, Shane E, de la Cruz L, Lindsay R, Bilezikian JP, Dempster DW. The histomorphometry of bone in primary hyperparathyroidism: preservation of cancellous bone structure. J Clin Endocrinol Metab 1990;70:930–938. [PubMed: 2318948]
42. Recker R, Lappe J, Davies KM, Heaney R. Bone remodeling increases substantially in the years after menopause and remains increased in older osteoporosis patients. J Bone Miner Res 2004;19:1628–1633. [PubMed: 15355557]
43. Recker R, Masarachia P, Santora A, Howard T, Chavassieux P, Arlot M, Rodan G, Wehren L, Kimmel D. Trabecular bone microarchitecture after alendronate treatment of osteoporotic women. Curr Med Res Opin 2005;21:185–194. [PubMed: 15801989]
44. Recker, RR.; Barger-Lux, MJ. Transilial bone biopsy. In: Bilezikian, JP.; Raisz, LG.; Rodan, GA., editors. Principles of Bone Biology. Academic Press; San Diego, CA: p. 1625-1634.
45. Riggs BL, Melton LJ, Robb RA, Camp JJ, Atkinson EJ, McDaniel L, Amin S, Rouleau PA, Khosla S. A population-based assessment of rates of bone loss at multiple skeletal sites: evidence for substantial trabecular bone loss in young adult women and men. J Bone Miner Res 2008;23:205–214. [PubMed: 17937534]
46. Rubin, MR.; Dempster, DW.; Sliney, J.; Compito, C.; Müller, R.; Paschalis, EP.; Roschger, P.; Zoehrer, R.; Klaushofer, K.; Zhou, H.; Kohler, T.; Silverberg, SJ.; Bilezikian, JP. Indices of Bone Quality Are Markedly Abnormal in Hypoparathyroidism; American Society for Bone and Mineral Research 28th Annual Meeting; Philadelphia, PA. 2006; AND JBMR IN PRESS
47. Ruegsegger P, Koller B, Muller R. A microtomographic system for the nondestructive evaluation of bone architecture. Calcif Tissue Int 1996;58:24–29. [PubMed: 8825235]
48. Sornay-Rendu E, Boutroy S, Munoz F, Delmas PD. Alterations of cortical and trabecular architecture are associated with fractures in postmenopausal women, partially independent of decreased BMD measured by DXA: the OFELY study. J Bone Miner Res 2007;22:425–433. [PubMed: 17181395]
49. Uchiyama T, Tanizawa T, Muramatsu H, Endo N, Takahashi HE, Hara T. A morphometric comparison of trabecular structure of human ilium between microcomputed tomography and conventional histomorphometry. Calcif Tissue Int 1997;61:493–498. [PubMed: 9383277]
50. Van Rietbergen B, Odgaard A, Kabel J, Huiskes R. Direct mechanics assessment of elastic symmetries and properties of trabecular bone architecture. J Biomech 1996;29:1653–1657. [PubMed: 8945668]
51. Zysset PK, Guo XE, Hoffler CE, Moore KE, Goldstein SA. Elastic modulus and hardness of cortical and trabecular bone lamellae measured by nanoindentation in the human femur. J Biomech 1999;32:1005–1012. [PubMed: 10476838]

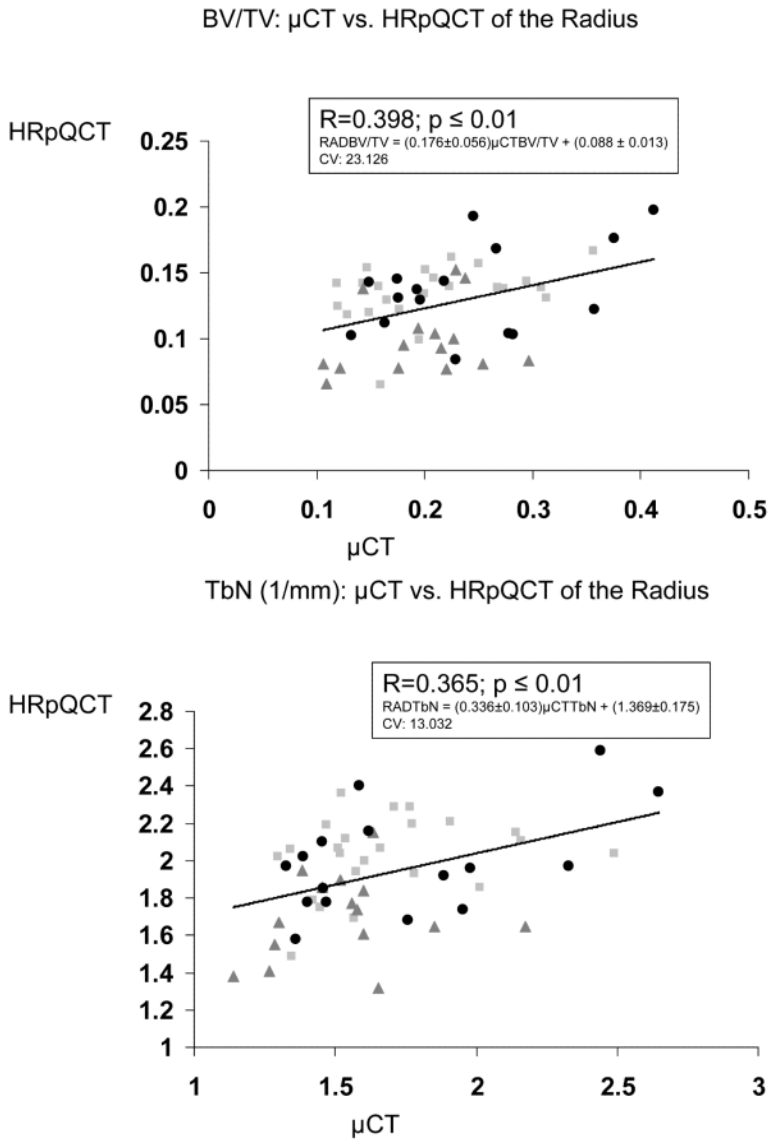

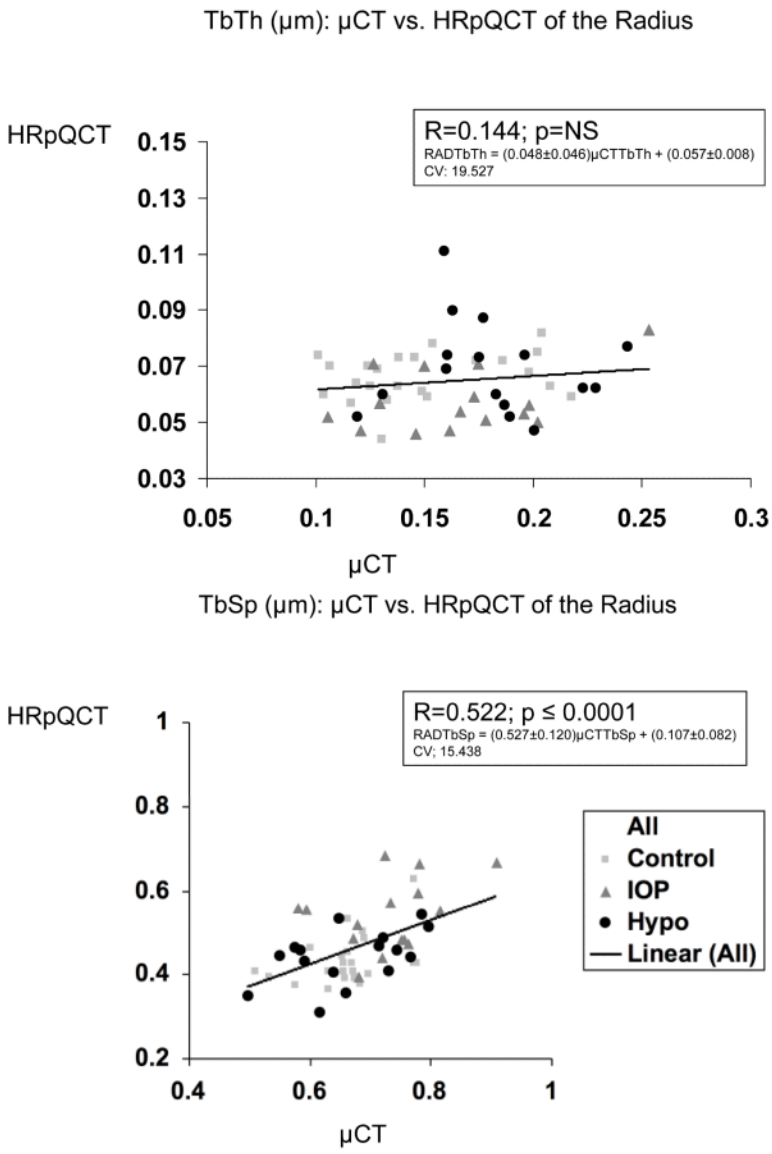

Figure 1.

Correlations (R) between trabecular parameters measured by µCT of biopsies and HR-pQCT of the radius. A. BV/TV , B. Tb.N. , C. Tb.Th. , and D. Tb.Sp. Square=premenopausal controls with normal BMD, Triangle = premenopausal women with IOP; Circle = men and women with hypoparathyroidism.

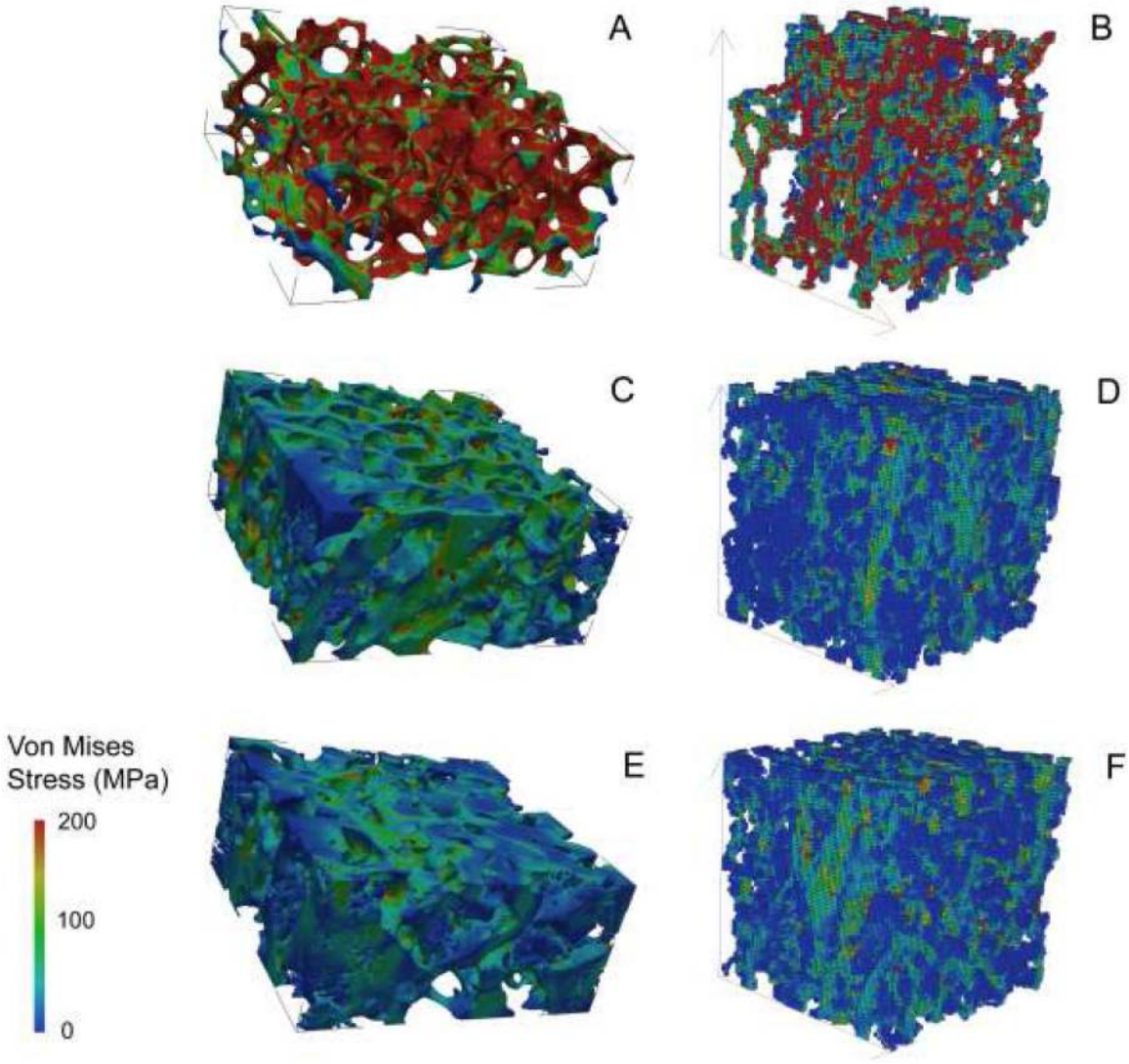

Figure 2.
Images showing von Mises stress were generated using μFE based on μCT of biopsies (A,C,E) and HR-pQCT (B,D,F) of the radius in a premenopausal woman with idiopathic osteoporosis (A and B), a normal premenopausal control (C and D), and a patient with hypoparathyroidism and unusually high bone density (E and F).

Table 1

Mean values ± SD for the analyzed variables

	Variable	Mean ± SD	Range
Age	Age (yrs)	39.3 ± 9.5	22-65
Areal Bone Mineral Density by DXA			
Lumbar Spine	Absolute BMD (g/cm^2)	1.067 ± 0.19	0.745 – 1.535
	T score	0.15 ± 1.70	−3.00 — 4.34
Total Hip	Absolute BMD (g/cm^2)	0.963 ± 0.18	0.600 – 1.448
	T score	0.11 ± 1.42	−2.80 — 4.15
Transiliac Biopsies			
2D Histomorphometry	BV/TV (%)	19.1 ± 5.3	9.0 - 30.8
	TbN (1/mm)	1.7 ± 0.3	1.0 - 2.3
	TbTh (μm)	113 ± 23	77 - 195
	TbSp (μm)	503 ± 135	317 - 955
	Cortical Width (μm)	835 ± 269	406 - 1561
3D mCT	BV/TV (%)	21.4 ± 7.11	10.6 - 41.3
	TbN (1/mm)	1.7 ± 0.3	1.1 - 2.7
	TbTh (μm)	164 ± 38	10 - 253
	TbSp (μm)	681 ± 83	498 - 908
HR-pQCT			
Radius	BV/TV (%)	12.6 ± 3.1	6.5 - 19.8
	TbN (1/mm)	1.9 ± 0.3	1.3 - 2.6
	TbTh (μm)	65 ± 13	44 - 111
	TbSp (μm)	465 ± 83	310 - 685
	Cortical Density (mg HA/cm^3)	910 ± 54	763 - 1018
	Cortical Thickness (μm)	825 ± 176	520 - 1260
Tibia	BV/TV (%)	13.0 ± 2.9	6.2 - 20.0
	TbN (1/mm)	1.9 ± 0.4	1.1 - 2.5
	TbTh (μm)	69 ± 10	49 - 109
	TbSp (μm)	478 ± 112	329 - 834
	Cortical Density (mg HA/cm^3)	903 ± 46	788 - 997
	Cortical Thickness (μm)	1133 ± 221	710 - 1670
Apparent Young's Moduli (MPa)			
HR-pQCT of Radius	E_{11} (medial-lateral)	335 ± 182	75 - 778
	E_{22} (anterior-posterior)	533 ± 314	56 - 1660
	E_{33} (longitudinal)	1018 ± 582	116 - 2664
HR-pQCT of Tibia	E_{11} (medial-lateral)	239 ± 127	59 - 572
	E_{22} (anterior-posterior)	345 ± 188	118 - 941
	E_{33} (longitudinal)	965 ± 416	341 - 2198

	Variable	Mean ± SD	Range
μCT of Biopsy	E (long axis of specimen)	660 ± 485	79 - 2165

Table 2

Relationships between trabecular and cortical microarchitectural parameters measured by 2D histomorphometry, μCT, HR-pQCT and areal BMD by DXA

	BV/TV	Tb.N	Tb.Th	Tb.Sp	Ct.Th
2D Hist vs 3D μCT: Iliac Crest	0.873 [c]	0.613 [c]	0.825 [c]	0.719 [c]	N/A [*]
HR-pQCT: Radius vs Tibia [**]	0.758 [c]	0.516 [c]	0.357 [b]	0.509 [c]	0.578 [c]
2D Hist Iliac Crest vs HR-pQCT Radius	0.304 [a]	0.243	0.058	0.264	0.003
2D Hist Iliac Crest vs HR-pQCT Tibia [**]	0.272	0.198	0.106	0.169	0.360 [b]
2D Hist Iliac Crest vs LS BMD	0.274 [a]	0.230	0.130	−0.239	0.254
2D Hist Iliac Crest vs TH BMD	0.306 [a]	0.214	0.104	−0.194	0.378 [b]
3D μCT Iliac Crest vs HR-pQCT Radius	0.398 [b]	0.365 [b]	0.144	0.522 [c]	N/A
3D μCT Iliac Crest vs HR-pQCT Tibia [**]	0.276 [a]	0.215	0.177	0.339 [b]	N/A
3D μCT Iliac Crest vs LS BMD	0.352 [b]	0.303 [a]	0.156	−0.413 [b]	N/A
3D μCT Iliac Crest vs TH BMD	0.365 [b]	0.218	0.247	−0.423 [b]	N/A

[*] N/A: Not available

[**] n=54 except for relationships involving HR-pQCT of the tibia where n=52

[a] $P \leq 0.05$

[b] $P \leq 0.01$

[c] $P \leq 0.0001$

Table 3

Finite Element Analysis: Relationship (R) between apparent Young's moduli (MPa) derived from μCT of transiliac crest biopsies in the long axis of the specimens and those derived from HR-pQCT scans (in three directions)

Finite Element Analysis	HR-pQCT Radius vs Tibia	Transiliac Biopsy vs HR-pQCT Radius	Transiliac Biopsy vs HR-pQCT Tibia
E_{11} (Medial-Lateral)	0.615 [c]	0.442 [b]	0.380 [b]
E_{22} (Anterior-Posterior)	0.372 [b]	0.332 [a]	0.181
E_{33} (Longitudinal)	0.380 [b]	0.372 [b]	0.115

[a] $P \leq 0.01$

[b] $P \leq 0.001$

[c] $P \leq 0.0001$